Pattern Recognition Letters 33 (2012) 2113–2119

Contents lists available at SciVerse ScienceDirect

Pattern Recognition Letters

journal homepage: www.elsevier.com/locate/patrec

On the generation and pruning of skeletons using generalized Voronoi diagrams

Hongzhi Liu [a,d], Zhonghai Wu [a,b,*], D. Frank Hsu [c], Bradley S. Peterson [d], Dongrong Xu [d]

[a] School of Electronics Engineering and Computer Science, Peking University, Beijing 100871, PR China
[b] School of Software and Microelectronics, Peking University, Beijing 102600, PR China
[c] Department of Computer and Information Science, Fordham University, New York, NY 10023, USA
[d] MRI Unit, Department of Psychiatry, Columbia University & New York State Psychiatric Institute, New York, NY 10032, USA

ARTICLE INFO

Article history:
Received 19 February 2012
Available online 28 July 2012

Communicated by G. Borgefors

Keywords:
Skeletonization
Generalized Voronoi diagram
Skeleton pruning
Reconstruction contribution
Visual contribution
Generalized Voronoi skeleton (GVS)

ABSTRACT

Skeletonization is a necessary process in a variety of applications in image processing and object recognition. However, the concept of a skeleton, defined using either the union of centers of maximal discs or the union of points with more than one generating points, was originally formulated in continuous space. When they are applied to situation in discrete space, the resulting skeletons may become disconnected and further works are needed to link them.

In this paper, we propose a novel skeletonization method which extends the concept of a skeleton to include both continuous and discrete space using generalized Voronoi diagrams. We also present a skeleton pruning method which is able to remove noisy branches by evaluating their significance. Three experimental results demonstrate that: (1) our method is stable across a wide range of shapes, and (2) it performs better in accuracy and robustness than previous approaches for processing shapes whose boundaries contain substantial noise.

1. Introduction

A "skeleton", also termed a "medial axis", is a compact and efficient representation of a shape or an object. Skeletonization is a process that transforms 2D shapes into skeleton graphs while preserving both the topology and geometry information of the original shape. We can reconstruct the original shape of a 2D object from its skeleton with the help of a radius function. These desirable properties of skeletonization have been used in diverse applications, such as object recognition and segmentation, image compression and retrieval, and analysis of scientific and medical images.

Since the first definition of a skeleton by Blum (1967), various methods have been proposed to extract skeletons from 2D shapes. These methods can be roughly classified into three types. The first type of methods is based on the extraction of centers of maximal disks (Remark A). However, the centers of maximal disks may not be connected in discrete space (Fig. 1a). Different methods have been proposed to extract and link the centers of maximal discs. Some excellent results in this direction have been obtained (Arcelli and Sanniti di Baja, 1993; Sanniti di Baja and Thiel, 1996; Ge and Fitzpatrick, 1996). The second type of methods simulates prairie fire model: assume that the object is homogeneously covered with dry grass and we set its boundary on fire, the locus where the fire fronts meet and quench is the skeleton. These methods iteratively remove the border points (i.e. thinning), or shrink or propagate the object contour to determine the skeleton (Zhang and Suen, 1984; Jang and Chin, 1990; Riazanoff et al., 1990; Leymarie and Levine, 1992; Kimmel et al., 1995; Costa, 2003). The iterative process is a time-consuming operation and several methods have been proposed to speed up the process (Arcelli and Sanniti di Baja, 1985; Costa and Manoel, 2001). A similar definition of prairie fire model uses the number of generating points (Remark B). Like the centers of maximal disks, this type of skeleton points may also be disconnected in discrete space (Fig. 1b). Several methods have been proposed to deal with this problem (Choi et al., 2003; Shen et al., 2011). The third type of methods extracts the skeleton using some mathematical or physical properties of a skeleton, such as methods based on Voronoi diagram (Kirkpatrick, 1979; Lee, 1982; Brandt and Algazi, 1992; Mayya and Rajan, 1994; Ogniewicz and Kübler, 1995; Fabbri et al., 2002), methods based on divergence theorem (Siddiqi et al., 2002; Dimitrov et al., 2003) and physics-based deformable models (Krinidis and Chatzis, 2009).

Remark A (*SK1*). Let F be a connected region in R^2. The maximal discs in F are the discs which fit inside F but not contained in any other disc that is also inside F. The *skeleton* of F is the union of the centers of all maximal discs in F (Blum and Nagel, 1978).

Remark B (*SK2*). Let F be a connected region in R^2, B be its boundary, i.e. $B = \partial F$, and p be a point in F. The *generating points* of p are defined as $\{q \in B | d(p,q) \leqslant d(p,m), \forall m \in B\}$. If p has more than one

* Corresponding author at: School of Electronics Engineering and Computer Science, Peking University, Beijing 100871, PR China. Tel.: +86 1061273696; fax: +86 1061273670.
E-mail addresses: wuzh@pku.edu.cn, wuzh@ss.pku.edu.cn (Z. Wu).

0167-8655/$ - see front matter © 2012 Elsevier B.V. All rights reserved.
http://dx.doi.org/10.1016/j.patrec.2012.07.014

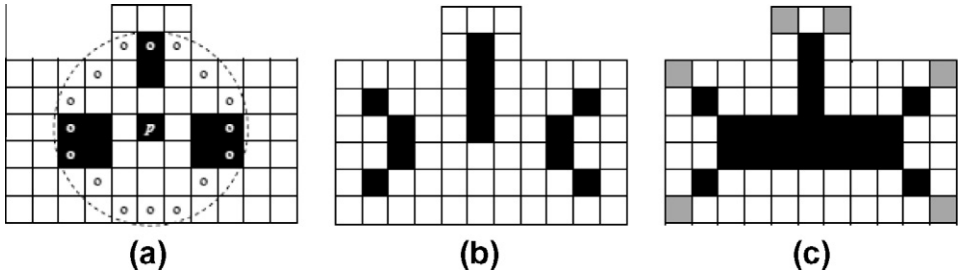

Fig. 1. Examples of discrete skeleton according to: (a) the center of maximal discs (Remark A, SK1), (b) the number of generating points (Remark B, SK2), and (c) generalized Voronoi skeleton (GVS) generated by our method. Blocks denote foreground pixels and the black and gray blocks denote skeleton pixels. The boundary pixels of the maximal disc centered at p are marked by 'o'. Gray blocks denote the salient points.

generating points, then p is a *skeletal point* of F. The union of all skeletal points of F is called the *skeleton* of F (Blum, 1967; Pavlidis, 1982).

In this paper, we propose a novel skeletonziation method using generalized Voronoi diagrams. The definition of a skeleton in continuous space (Remarks A and B) is extended to include discrete space. The extended skeleton, called generalized Voronoi skeleton (GVS), can ensure the connectedness of the skeleton when mapped into discrete space (Fig. 1c). To remove the insignificant branches that may be easily induced by boundary noise, we present a skeleton pruning method which evaluates the significance of each branch by both its reconstruction contribution (a global significant measurement) and visual perception contribution (a local significant measurement).

The rest of the paper is organized as follows. In Section 2, we define the concept of a generalized Voronoi skeleton (GVS) using the properties of salient points. In Section 3, we present an algorithm for skeletonization in the generation and pruning of GVS. Experimental results and discussion are presented in Section 4. In Section 5, we conclude with a summary and future works.

2. Salient points and generalized Voronoi skeleton

We extend the definition of SK1 (Remark A) so that it can divide the object region into sub-regions. The extended skeleton is the boundaries of these sub-regions, and skeletonization becomes a problem of subdividing object regions (Fig. 2). The main advantage of this new definition is that it can make sure the skeletons are still connected when mapped into discrete space.

In continuous space, the skeleton points on SK1 (Remark A) can be classified into three types according to the intersection set of their maximal discs and the object contour. The points whose maximal disc touches the object contour in two and only two separate and continuous sets of points are called *normal points*. The points whose maximal disc touches the object contour in three or more separate continuous sets are called *branch points*. And the points whose maximal disc touches the object contour in only one continuous set are *end points* (Blum and Nagel, 1978).

The maximal disc centered at each end point intersects the object contour with a circular curve segment (which may degrade to one point in some cases). We call the middle points of these circular curve segments *salient points* of the object contour (Definition 1). These salient points divide the object contour into several *contour curve segments*. If we extend SK1 by connecting its end points with their corresponding salient points, we get a new skeleton, which we call *generalized Voronoi skeleton* (GVS). GVS is composed of both SK1 and the extension line segments. Hence, it divides the object region into disjoint sub-regions (Fig. 2). Salient point and generalized Voronoi skeleton (GVS) are formally defined as follows.

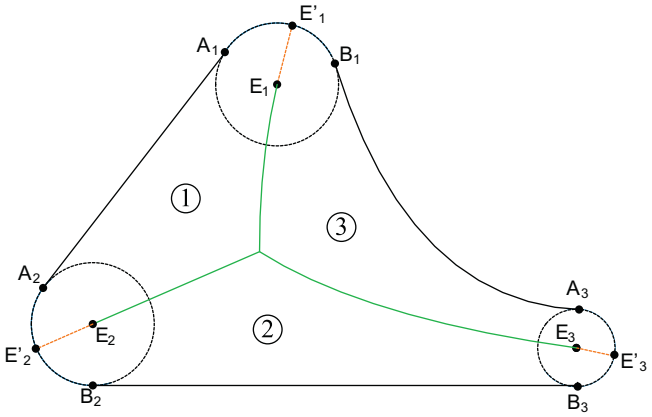

Fig. 2. Medial skeleton and generalized Voronoi skeleton. $E_i (i = 1,2,3)$ are the endpoints of conventional medial skeleton (green lines). A_iB_i are the intersection curve segments of the object contour and the maximal disc centered at E_i, E_i' are the salient points which are the middle points of $\widehat{A_iB_i}$. The generalized Voronoi skeleton (GVS) is the union of the medial skeleton (green lines) and the connecting lines (red dash lines) that connect each endpoint with its corresponding salient point. GVS divides the object region into three sub-regions ①, ②, and ③. (For interpretation of the references to color in this figure legend, the reader is referred to the web version of this article.)

Definition 1 (Salient Point). A point p on the object contour ∂F is called a *salient point* if it satisfies one of the following conditions:

(1) Point p is a convex vertex ('vertex' means that there is no definition of curvature at point p).
(2) Point p is a point with local maximal curvature, i.e., there exists a neighborhood of p, $N(p) \subset \partial F$, such that $\kappa(p) > \kappa(q)$, for $q \in N(p)$ and $q \neq p$, where $\kappa(p)$ and $\kappa(q)$ are the curvature value at p and q separately.
(3) Point p is the middle point of a maximally extended convex circular curve segment ('Convex circular' means the curvature at all points on this curve segment are the same and positive. 'Maximally extended' means the curvature at the two neighbor points at its two ends of the circular curve segment are different from that at points on the curve segment).

GVS can be seen as a subset of the generalized Voronoi boundaries by taking the contour curve segments connected by the *salient points* as sites (Definition 2). Let O be a set of n distinct points (called sites) in the plane. The Voronoi diagram of O is the subdivision of the plane into n cells, one for each site. A point p lies in the cell corresponding to a site $o_i \in O$ if and only if the distance between p and o_i is smaller than that between p and any other site o_j, $i \neq j$. For generalized Voronoi diagrams, the sites can be other shapes besides points, such as line segments and curves.

Definition 2 (GVS). Let ∂F be the contour of the object region F, sp_i ($i = 1,\ldots,n$) be the *salient points* of ∂F, $S = \{S_1, S_2, \ldots, S_n\}$ be the set of *contour curve segments* on ∂F connected by $sp_i (i = 1,\ldots,n)$, $C = \{C_1, C_2, \ldots, C_n\}$ be the generalized Voronoi cells of S, and $\partial C = \partial C_1 \cup \partial C_2 \cup \ldots \cup \partial C_n$ be the generalized Voronoi boundaries of S. The *generalized Voronoi skeleton* of F is the subset of generalized Voronoi boundaries of S that are inside F, i.e. $\{p | p \in F \cap \partial C\}$.

When mapped into discrete space, GVS remains to be connected (Fig. 1c).

3. Algorithm for skeletonization

Based on Definition 2, we design an algorithm to extract GVS. First, we locate the salient points (Section 3.1). Then, the generalized Voronoi diagram of the contour curve segments connected by salient points is computed and the generalized Voronoi boundaries inside the shape region are extracted, which then form the generalized Voronoi skeleton (Section 3.2). At last, we remove the insignificant branches by a pruning method which takes into consideration both the reconstruction and visual contributions of each branch (Section 3.3).

3.1. Detection of salient points

In continuous space, we can locate the salient points using the curvature information according to Definition 1. In discrete space, when we deal with digital images, the object contour is always defined as a sequence of points. According to Definition 1, every convex vertex should be a salient point. However, many of them are false salient points that may be caused by noise or digitalization. Different methods have been developed for detecting the true salient points on discrete contour curves (Teh and Chin, 1989; Perez and Vidal, 1994; Latecki and Lakämper, 1999; Carmona-Poyato et al., 2010). The discrete curve evolution (DCE) method (Latecki and Lakämper, 1999; Bai et al., 2007) has been shown to be superior because of its ability to process false salient points.

The main idea of DCE is to iteratively remove a vertex with the smallest relevance value, which reflects the visual significance of the vertex (Latecki and Lakämper, 1999). Let E_1 and E_2 be the two edges adjacent to a vertex P_i, i.e. $E_1 = \overline{P_{i-1}P_i}$, $E_2 = \overline{P_iP_{1+1}}$. We define the relevance value of P_i as:

$$K(P_i) = \frac{\beta(E_1, E_2) l(E_1) l(E_2)}{l(E_1) + l(E_2)},$$

where $\beta(E_1,E_2)$ is the turning angle from vector $\overline{P_{i-1}P_i}$ to vector $\overline{P_iP_{1+1}}$, and l is the length function normalized with respect to the length of the whole contour curve. In general, larger K values denote greater relevance or visual significance, and the associated vertices need to be retained. For example, consider two neighboring edges with known length, smaller turning angles between them denote smoother transitions, corresponding to insignificant shape parts that can be removed; whereas larger turning angles indicate more prominent shape parts. On the other hand, when the lengths of the edges are small, K is also small, indicating local small twigs, whereas edges with large length indicate major shape parts. An important property of DCE is that it can generate a hierarchical abstract of the original shape at different levels of details (Latecki and Lakämper, 1999).

Although DCE can efficiently remove most of the noise and insignificant vertices, it may remove some significant salient points (corresponding to significant skeleton branches) prior to the removal of the targeted insignificant ones. Therefore, we only use DCE to remove most of the false salient points. Then we use a new pruning technique (Section 3.3) to remove the insignificant branches induced by the remaining false salient points.

3.2. Extracting the generalized Voronoi skeleton

Let ∂F denote the contour of the foreground region F, sp_i ($i = 1,\ldots,n$) be the salient points of ∂F, and $S = \{S_1, S_2, \ldots, S_n\}$ be the set of curve segments on ∂F connected by sp_i. If we take $\{S_i\}$ as sites, then the corresponding generalized Voronoi cells of S inside F are defined as:

$$C(S_i) = \{p \in F | d(p, S_i) \leqslant d(p, S_j),\ \forall S_j \in S\} = \{p \in F | d(p, S_i) = d(p, \partial F)\}, \quad S_i \in S.$$

The distance between a point p and a curve segment S_i is defined as the shortest distance between p and the points belong to S_i, i.e. $d(p,S_i) = \min\{d(p,q) | q \in S_i\}$. $C(S_i)$ is the set of points whose distance to S_i is not larger than that to any other curve segment in S. According to Definition 2, the generalized Voronoi skeleton of F is the boundaries of these generalized Voronoi cells.

Assume that p is a point in F, and q is the projection of p on ∂F, such that $d(p,q) = d(p,\partial F)$, we call q the *generating point* of p and the curve segment S_j, which contains q, is called the *generating site* of p. All points with the same generating site are grouped into a separated region which corresponds to a generalized Voronoi cell.

The *generating point map*, whose value for each point in F is the index of the closest point on ∂F, can be thought as a by-product of a modified distance transform (Fabbri et al., 2008):

$$D'(p) = d(p, F'^c) = \min\{d(p,q) | q \in F'^c\},$$

Where $F' = F \setminus \partial F = \{p | p \in F,\ p \notin \partial F\}$, and $F'^c = I \setminus F'$, I denotes the whole image regions.

For each point p in F, we have $D'(p) = d(p, F'^c) = d(p, \partial F) = \min\{d(p,q) | q \in \partial F\}$. We can get the generating point map by recording the closest contour point for each point in F during the process of computing the distance transform map (Maurer et al., 2003). Then the *generating site map* can be computed by a simple transformation which maps the indices of contour points to the indices of their corresponding contour curve segments. Given the generating site map, we can easily compute the GVS by an edge detection operator.

The generalized Voronoi skeleton generated by previous steps may be not unit pixel width (Fig. 1c). A one-pixel width skeleton can be obtained by an iteration of thinning (Zhang and Suen, 1984; Jang and Chin, 1990).

3.3. Pruning based on reconstruction and visual contributions

Using DCE to detect the salient points, we can efficiently remove most of the noisy and insignificant vertices. However, to make sure all significant salient points are not removed, some insignificant salient points are also retained, each of which will induce an insignificant branch (see Section 2).

To remove the insignificant branches, we propose a pruning technique that measures the significance of a branch based on: (1) its reconstruction contribution (RC), which is measured by the residual shape area—the area that can only be reconstructed by this branch (gray region part in Fig. 3a)—relative to the whole shape area, and (2) its visual contribution (VC), which is measured by the length of residual part of the skeleton branch—the part that is not contained in the maximal disc centered at the adjacent branch point (red line in Fig. 3a)—relative to the radius of the maximal disc centered at the adjacent branch point (Fig. 3a). The reconstruction contribution is a global measurement, while the visual contribution is a local measurement. Both of these two measurements are invariant under translation, rotation and scaling.

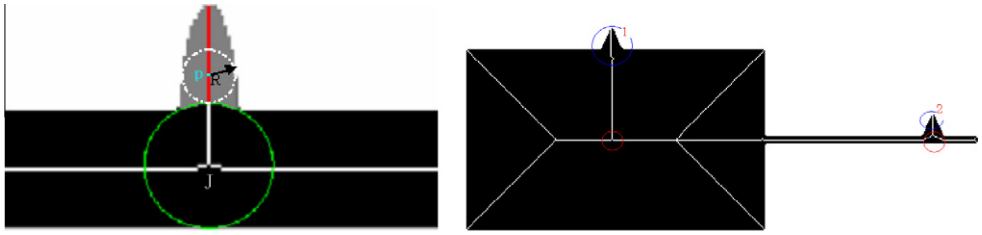

Fig. 3. Measurements and effects of reconstruction and visual contributions. (a) On left, an example of the residual part of a skeleton branch. The red line is the residual part of the branch. The gray part is the residual shape area for the skeleton branch as it can only be reconstructed by this branch. (b) On right, effects of two bumps with the same size but located at different places (indicated by the blue circles). According to reconstruction contribution, Bump 1 is more significant than Bump 2, while Bump 2 is more significant than Bump 1 by using visual contribution. (For interpretation of the references to color in this figure legend, the reader is referred to the web version of this article.)

The reconstruction contribution, as a global significance measurement, is insensitive to noise, but it may take some significant branches corresponding to thin region parts as insignificant ones (Fig. 3b). Visual contribution, as a local significance measurement, is context-aware. However, it may take some branches that have large reconstruction contributions, which is an important property for skeleton, as insignificant branches. To take the advantages of these two significance measurements and avoid their disadvantages, we use them together and only remove the branches which have little contribution for both reconstruction and visual perception.

Based on these two significance measurements and proper threshold values, we can remove the insignificant branches induced by the insignificant salient points retained by DCE, as these branches have both little reconstruction and visual contributions.

4. Experiments

To evaluate the performance of the proposed skeletonization and pruning method, we test and compare it with other existing methods using silhouette images of both complex natural shapes and simple simulated shapes. We first examine the stability of the proposed method for different kinds of object shapes. Then we compare the method with other state-of-art approaches both visually and quantitatively.

4.1. Parameter setting

Three parameters may affect the experimental results: N, the number of vertices in the simplified boundary polygon generated by DCE; t_{RC}, the threshold for reconstruction contribution; t_{VC}, the threshold for visual contribution (Section 3.3). To avoid DCE removing any salient vertices belonging to significant branches, we need to choose a large value for N. In all our experiments, we set the default value of N to be 30, which is shown large enough from our experiment results. To ensure the reconstruction ability of the final skeletons, we suggest setting t_{RC} not larger than 1%. In our experiments, we set the default value of t_{RC} used during pruning to be 1/400, i.e. 0.25%. To avoid removing some significant branches which have small reconstruction contribution but great visual contribution, we set the default value of t_{VC} *to be* 0.5.

4.2. Stability experiment

In this experiment, we test the stability of our method for different object shapes.

4.2.1. Experiment design

We use the complex natural shapes from the MPEG-7 Core Experiment CE-Shape-1 database (Latecki et al., 2000) as our testing set. There are 70 groups of objects with 20 different shapes in each group in this MPEG-7 dataset. In addition to visual inspection, we also quantitatively measure the reconstruction error of each skeletonization result by contrasting the reconstructed shape with the original shape and calculated the percentage of the areas that are under-reconstructed respected to the whole area of the original shape.

4.2.2. Results

Experiment results show that the skeletons generated by our method for the objects of the same class (e.g. shapes of two birds) are similar, although the objects may have different shapes (Fig. 4). The reconstruction test demonstrated that our method generates a small reconstruction error about 1%.

4.3. Pruning experiment

In this experiment, we compare the performance of our pruning method with one of the popularly used methods proposed by Bai et al. (2007).

4.3.1. Experiment design

We use a shape of horse as test data and computed its skeleton using either our method or Bai et al.'s method with different control parameters. We compare the generated results using these two methods to examine the improvement that our method could offer over the counterpart.

4.3.2. Results

Compared to Bai et al.'s method (2007), our method ensures to remove only the insignificant branches first, such as the head top branch of the horse in Fig. 5.

4.4. Quantitative comparison experiment

In this experiment, we use a simple rectangular shape to quantitatively compare the performance of our method with two other popular methods. This comparison is considered as a standard approach for investigating the performance of skeletonization methods (Krinidis and Chatzis, 2009).

4.4.1. Experimental design

We first select a simple rectangular shape whose skeleton is well known as gold-standard. Then we add different amount of boundary noise to this shape and use the noisy shapes as our testing samples (Fig. 6). For fairness, we test the same rectangles with the same noise as used in Shen et al. (2011) and Krinidis and Chatzis, 2009, and the same error measurement:

$$\mathrm{Err}(S,D)=\frac{1}{N}\sum_{i=1}^{N}\sqrt{(S_x(i)-D_x(i))^2+(S_y(i)-D_y(i))^2},$$

where S is the skeleton under consideration, D is the gold-standard skeleton, N is the number of skeleton points in S, $[S_x(i), S_y(i)]$ is the

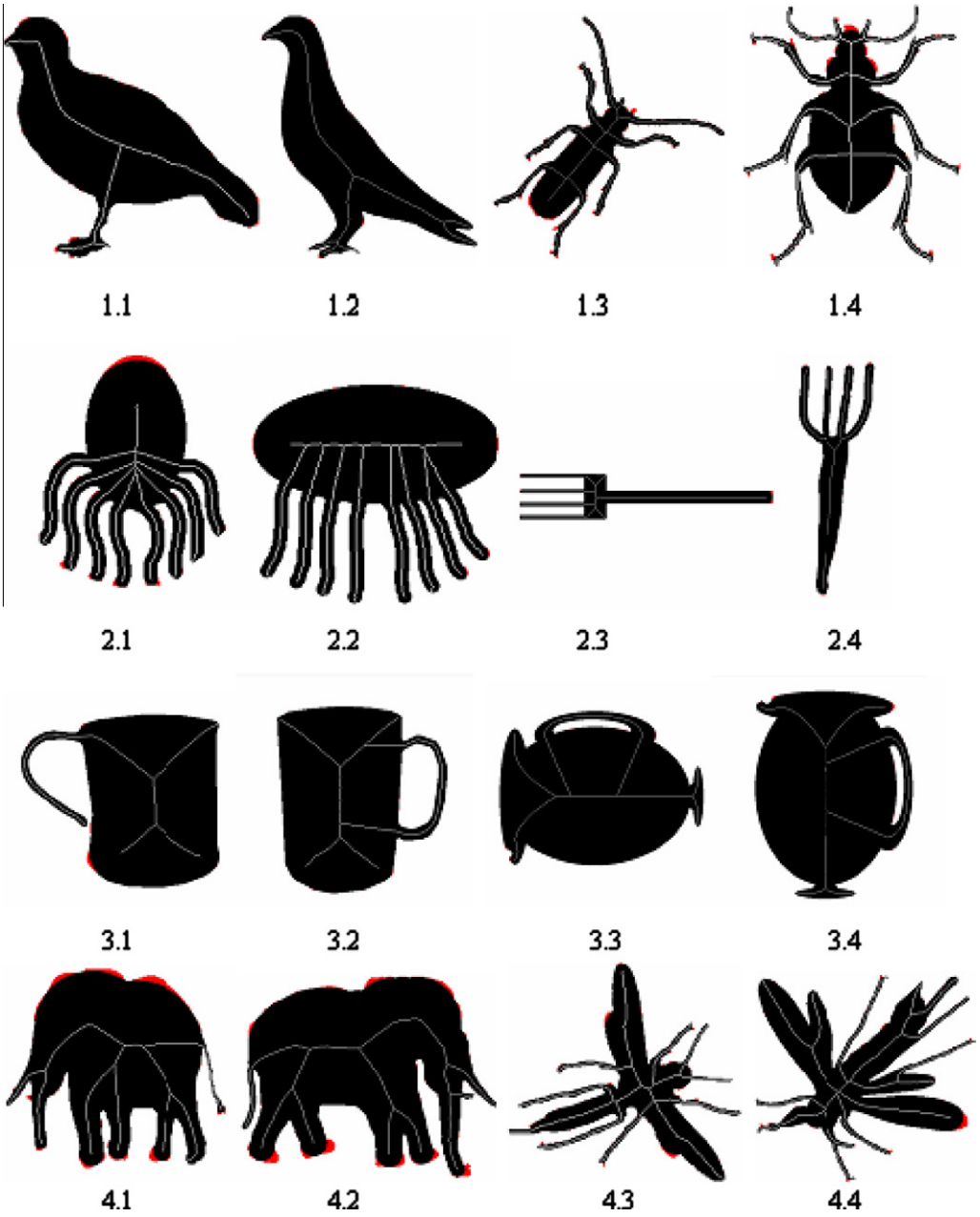

Fig. 4. Representative results using our method for different shapes of different objects in MPEG-7 shape dataset. Eight pairs of different shapes of the same object are presented. Our method generated similar skeletons for similar objects although their original shapes varied. The red regions indicate reconstruction errors, i.e. the difference between the reconstructed shape and the original shape. (For interpretation of the references to color in this figure legend, the reader is referred to the web version of this article.)

coordinate of the ith skeleton point in S and $[D_x(i), D_y(i)]$ is the closest point in D to the point $[S_x(i), S_y(i)]$.

4.4.2. Results

Experiment results show that our method is more accurate and robust than the other two methods, with an improvement of about 32% over Shen et al.'s approach (Shen et al., 2011) and about 45.2% over Krinidis et al.'s approach (Krinidis and Chatzis, 2009) (Table 1).

4.5. Discussion

Several other works, such as (Kirkpatrick, 1979; Lee, 1982; Brandt and Algazi, 1992; Mayya and Rajan, 1994; Ogniewicz and Kübler, 1995; Fabbri et al., 2002), also use the concept of Voronoi diagram and generalized Voronoi diagram for skeletonization. These methods use only points and straight line segments as sites. They approximate the contour of the original shape using a set of points or line segments as the initial step. Therefore they produce skeletons of the approximated shape instead of the original one (Székely, 2008). In contrast, our method directly takes curve segments of the original contour as sites to ensure the accuracy of the extracted skeleton. Although we ignore some salient points which we thought insignificant as they may be caused by noise or discretization (Section 3.1), this only removes the corresponding branches and will not affect the rest of the skeleton.

Relating to the definition of salient points, Leyton (Leyton, 1987) has explored the symmetry-curvature duality, which implies that every contour point with local maximal curvature (the same

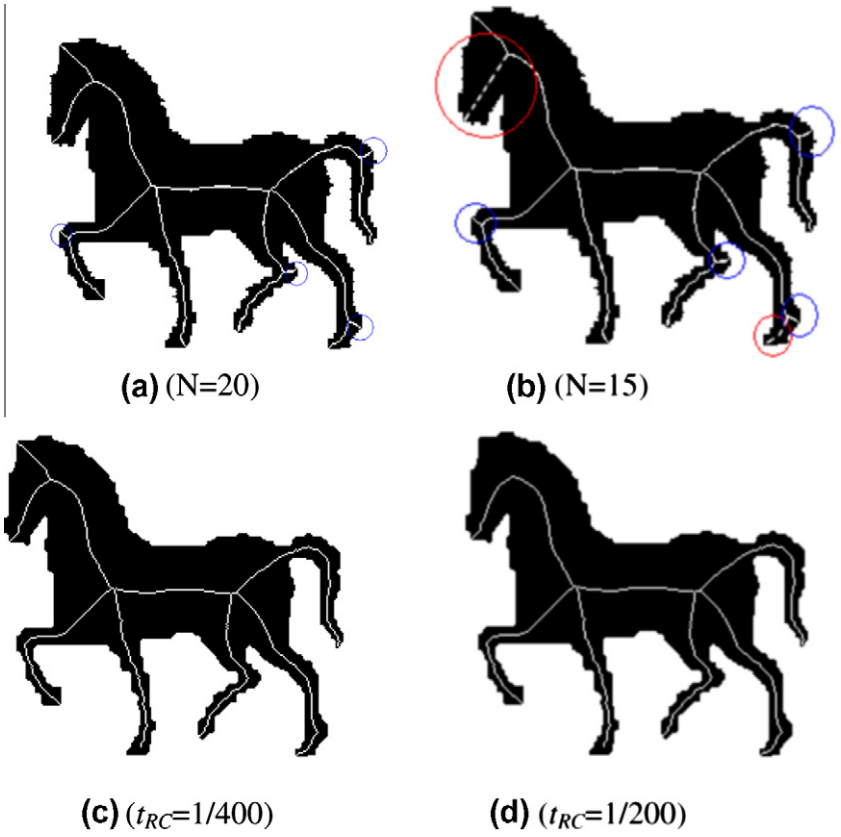

Fig. 5. Comparison between the results by Bai et al.'s method ((a) and (b)) and ours ((c) and (d)) for the same shape. The blue circles indicate the insignificant branches retained by Bai et al.'s DCE and the red circles indicate the significant skeleton branches removed by Bai et al.'s DCE prior to removing some insignificant branches. In contrast, our method can correctly process these portions. It successfully removed the insignificant branches in the first place as t_{RC} value increased. (For interpretation of the references to color in this figure legend, the reader is referred to the web version of this article.)

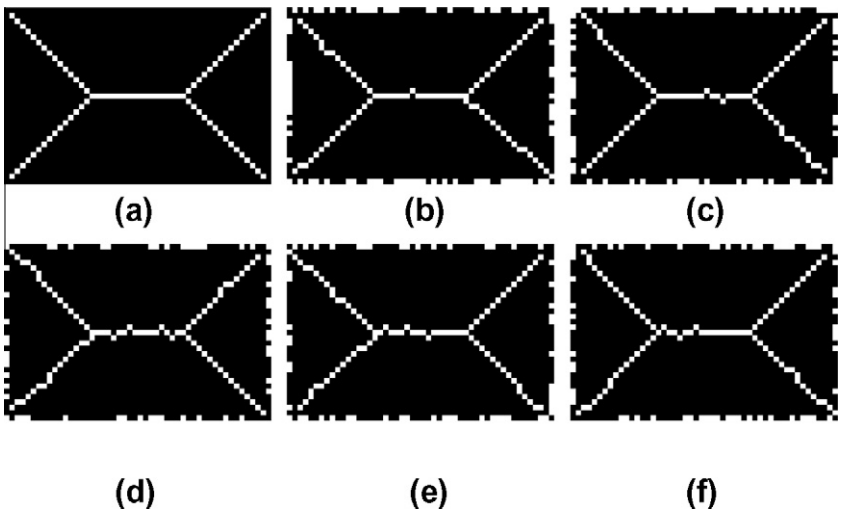

Fig. 6. Skeletons generated by our method using noisy rectangular shapes: (a) the original object (gold standard); (b) the object with Gaussian noise (0, 1.0) on its boundary; (c) with Gaussian noise (0, 1.2); (d) with uniform noise (1.0); (e) with uniform noise (1.2); (f) with uniform noise (1.5).

as the type 2 salient point in Definition 1) should be corresponding to a skeleton branch. Riazanoff et al. (1990), Kimmel et al. (1995), and Cesar and Costa (1999) used the symmetry–curvature duality to extract the skeleton in discrete space. Riazanoff et al. (1990) used a measurement of convexity to approximate the curvature of each contour pixel and extract the skeleton by curve translating (a process simulating the grassfire). Kimmel et al. (1995) approximated the curvature using central difference approximation (a technique very sensitive to noise). The authors aimed to reduce the effect of noise by smoothing the region at first. After locating the local maximal curvature points, the skeleton was extracted using level set. Cesar and Costa (1999) estimated the curvature using Fourier transformation (Cesar and Costa, 1996) and extracted the skeleton as $\xi(t) = \frac{u_l(t)+u_r(t)}{2}$, where $u_l(t)$ and $u_r(t)$ denote a pair of

Table 1
A comparison of the skeleton error with other methods for noisy images with known ground-truth in Fig. 6. The standard deviation of Shen's method was not reported in (Shen et al. 2011).

	Krinidis and Chatizs (2009)	Shen et al. (2011)	Our method
Average error (S, D)	0.31	0.25	0.17
St. dev.	0.02	—	0.03

matched contour segments. This method has been shown efficient for the extraction of neural bendrograms, which is an important problem for neural shape analysis (Cesar and Costa, 1999). Different from these methods, we remove the assumption that contour curve is smooth in continuous space (Definition 1). In discrete space, we believe every convex vertex is a salient point (type 1 in Definition 1). To remove the false positive cases that may be caused by noise or discretization, we adopt an efficient technique to detect the salient points (Section 3.1). In addition, we incorporate into this method a new pruning method that can efficiently remove the insignificant branches to get a concise skeleton in shape analysis and matching.

5. Conclusions and future works

In this paper, we extend the definition of a skeleton to solve the disconnection problem inherited by previous definitions based on maximal discs or generating points when mapped into discrete space. The extended skeleton, called Generalized Voronoi Skeleton (GVS), is the generalized Voronoi boundaries by taking the contour curve segments generated by contour partitioning as sites. We present an algorithm to extract GVS and a new approach for skeleton pruning that removes insignificant skeleton branches by evaluating both the reconstruction and visual contributions of each branch. Experimental results using complex natural shapes from MPEG-7 dataset showed that our method is robust to shape deformation, which is a highly desired feature for skeletonization. Comparisons with other state-of-art approaches using simulated shapes with known ground truth demonstrated that our method offers relatively more accurate and robust performance.

In our future work, we will seek some other algorithms to detect the salient points. In addition, we will design effective methods to combine the two significant measurements of visual contribution and reconstruction contribution.

Acknowledgement

This work is supported in part by China Scholarship Council (CSC), and National Key Technology R&D Program of China (2012BAH06B01 and 2012BAH18B04).

References

Arcelli, C., Sanniti di Baja, G., 1985. A width-independent fast thinning algorithm. IEEE Trans. Pattern Anal. Machine Intell. 7 (4), 463–474.
Arcelli, C., Sanniti di Baja, G., 1993. Euclidean skeleton via centre-of-maximal-disc extraction. Image Vision Comput. 11 (3), 163–173.
Bai, X., Latecki, L.J., Liu, W.Y., 2007. Skeleton pruning by contour partitioning with discrete curve evolution. IEEE Trans. Pattern Anal. Machine Intell. 29 (3), 449–462.
Blum, H., 1967. A transformation for extracting new descriptors of shape, models for the perception of speech and visual form. MIT Press, Cambridge, Mass., pp. 363–380.
Blum, N., Nagel, R.N., 1978. Shape description using weighted symmetric axis features. Pattern Recognit. 10 (3), 167–180.
Brandt, J.W., Algazi, V.R., 1992. Continuous skeleton computation by Voronoi diagram. Comput. Vision Graphics Image Process. 55 (3), 329–338.
Carmona-Poyato, A., Madrid-Cuevas, F.J., Medina-Carnicer, R., Muñoz-Salinas, R., 2010. Polygonal approximation of digital planar curves through break point suppression. Pattern Recognit. 43 (1), 14–25.
Cesar, R.M., Costa, L. Da F., 1996. Towards effective planar shape representation with multiscale digital curvature analysis based on signal processing techniques. Pattern Recognit. 29, 1559–1569.
Cesar, R.M., Costa, L. Da F., 1999. Computer-vision-based extraction of neural dendrograms. J. Neurosci. Methods 93, 121–131.
Choi, W.P., Lam, K.M., Siu, W.C., 2003. Extraction of the Euclidean skeleton based on a connectivity criterion. Pattern Recognit. 36, 721–729.
Costa, L. Da F., 2003. Enhanced multiscale skeletons. Real-Time Imaging 9 (5), 315–319.
Costa, L. Da F., Manoel, E.T.M., 2001. Optimized approach to multiscale skeleton generation. Opt. Eng. 40 (9), 1752–1753.
Dimitrov, P., Damon, J.N., Siddiqi, K., 2003. Flux invariants for shape. In: Proc. Conf. on Computer Vision and Pattern Recognition (CVPR'03), pp. 835–841.
Fabbri, R.L., Estrozi, F., Costa, L.F., 2002. On Voronoi diagrams and medial axes. J. Math. Imaging Vis. 17, 27–40.
Fabbri, R., Costa, L. Da F., Torelli, J.C., Bruno, O.M., 2008. 2D Euclidean distance transform algorithms: A comparative survey. ACM Comput. Surv. 40 (1), 1–44.
Ge, Y., Fitzpatrick, J.M., 1996. On the generation of skeletons from discrete Euclidean distance maps. IEEE Trans. Pattern Anal. Machine Intell. 18 (11), 1055–1066.
Jang, B.K., Chin, R.T., 1990. Analysis of thinning algorithms using mathematical morphology. IEEE Trans. Pattern Anal. Machine Intell. 12 (6), 541–551.
Kimmel, R., Shaked, D., Kiryati, N., Bruckstein, A.M., 1995. Skeletonization via distance maps and level sets. Comput. Vision Image Understanding 62, 382–391.
Kirkpatrick, D.C., 1979. Efficient computation of continuous skeletons. In: IEEE 20th Ann. Symp. on Foundations of Computer Science, pp. 18–27.
Krinidis, S., Chatzis, V., 2009. A skeleton family generator via physics-based deformable models. IEEE Trans. Image Process. 18 (1), 1–11.
Latecki, L.J., Lakamper, R., Eckhardt, U., 2000. Shape descriptors for non-rigid shapes with a single closed contour. In: Proc. Conf. on Computer Vision and Pattern Recognition (CVPR).
Latecki, L.J., Lakämper, R., 1999. Convexity rule for shape decomposition based on discrete contour evolution. Comput. Vision Image Understanding 73 (3), 441–454.
Lee, D.T., 1982. Medial axis transformation of a planar shape. IEEE Trans. Pattern Anal. Machine Intell. 4 (4), 363–369.
Leymarie, F., Levine, M.D., 1992. Simulating the grassfire transform using an active contour model. IEEE Trans. Pattern Anal. Machine Intell. 14 (1), 56–75.
Leyton, M., 1987. Symmetry–curvature duality. Comput. Vision Graphics Image Process. 38, 327–341.
Maurer, C.R., Qi, R., Raghavan, V., 2003. A linear time algorithm for computing exact Euclidean distance transforms of binary images in arbitrary dimensions. IEEE Trans. Pattern Anal. Machine Intell. 25 (2), 265–270.
Mayya, N., Rajan, V.T., 1994. Voronoi diagrams of polygons: A framework for shape representation. In: Proc. Conf. on Computer Vision and Pattern Recognition (CVPR'94), pp. 638–643.
Ogniewicz, R.L., Kübler, O., 1995. Hierarchic Voronoi skeletons. Pattern Recognit. 28 (3), 343–359.
Pavlidis, T., 1982. Algorithms for Graphics and Image Processing. Springer-Verlag, Berlin, Heidelberg, New York.
Perez, J.C., Vidal, E., 1994. Optymum polygonal approximation of digitized curves. Pattern Recognition Lett. 15, 743–750.
Riazanoff, S., Cervelle, B., Chorowicz, J., 1990. Parametrisable skeletonization of binary and multilevel images. Pattern Recognition Lett. 11, 25–33.
Sanniti di Baja, G., Thiel, E., 1996. Skeletonization algorithm running on path-based distance maps. Image Vision Comput. 14, 47–57.
Shen, W., Bai, X., Hu, R., Wang, H.Y., Latecki, L.J., 2011. Skeleton growing and pruning with bending potential ratio. Pattern Recognit. 44 (2), 196–209.
Siddiqi, K., Bouix, S., Tannenbaum, A., Zucker, S.W., 2002. Hamilton–Jacobi skeletons. Internat. J. Comput. Vision 48 (3), 215–231.
Székely, G., 2008. Voronoi skeletons. In: Siddiqi, K., Pizer, S.M. (Eds.), Medial Representations: Mathematics, Algorithms and Applications. Springer, Berlin, Germany, pp. 191–221.
Teh, C.H., Chin, R.T., 1989. On the detection of dominant points on digital curves. IEEE Trans. Pattern Anal. Machine Intell. 11 (8), 859–872.
Zhang, T.Y., Suen, C.Y., 1984. A fast parallel algorithm for thinning digital patterns. Commun. ACM 27, 236–239.